Journal of Power Sources 196 (2011) 8064–8072

Contents lists available at ScienceDirect

Journal of Power Sources

journal homepage: www.elsevier.com/locate/jpowsour

On the essential role of current density in electrocatalytic activity of the electrodeposited platinum for oxidation of ammonia

C. Zhong [a], W.B. Hu [a,*], Y.F. Cheng [b,**]

[a] State Key Laboratory of Metal Matrix Composites, Shanghai Jiao Tong University, Shanghai 200240, China
[b] Dept. of Mechanical and Manufacturing Engineering, University of Calgary, Calgary, AB T2N 1N4, Canada

ARTICLE INFO

Article history:
Received 10 April 2011
Received in revised form 19 May 2011
Accepted 21 May 2011
Available online 27 May 2011

Keywords:
Ammonia oxidation
Platinum electrocatalysts
Electrolytic deposition
Electrocatalytic activity
Current density

ABSTRACT

Fabrication by electrolytic deposition of platinum (Pt) electrocatalyst provides a promising alternative for oxidation of ammonia. This work investigated the role of current density in the electrocatalytic activity of the prepared Pt electrocatalysts by cyclic voltammetry and surface characterization. The Pt loading amount is determined by inductively coupled plasma. Results demonstrated that, the electrodeposited Pt has a much higher electrocatalytic activity than the pure Pt electrode due to the high electroactive surface area of the Pt deposit. The electrocatalytic activity of the Pt catalyst is improved with the increase of the Pt loading. Moreover, the electrocatalytic activity of Pt increases with the depositing current density which results in an increasing Pt loading amount. The depositing current density also affects the surface morphology of the prepared Pt. The high depositing current density generates small Pt particles at a nanometer scale, or sheet-like dendritic structure. However, the low current density leads to large Pt particles at several hundreds of nanometer with a relatively smooth morphology. The Pt electrocatalyst with the former morphological feature exhibits a higher electrocatalytic activity than the later due to the higher electroactive surface area.

1. Introduction

Electro-oxidation of ammonia has been paid much attention in recent years from both ecological and energetic aspects [1–5]. While ammonia-containing wastewaters have detrimental effects on environment, ammonia serves as a potential fuel for direct fuel cell technologies [6,7] as well as an excellent hydrogen carrier [8]. Liquid ammonia contains 1.7 times more hydrogen and boasts a specific energy density 50% higher than liquid hydrogen for a given volume [8]. Electro-oxidation of ammonia has been approved to be an effective alternative for production of hydrogen [1,2,9–13].

Platinum (Pt) and its alloys have been acknowledged to own unparalleled advantages over other noble metals for catalytic electro-oxidation of ammonia [11–13]. However, Pt, as a rare resource, is not economic to be used for the electrocatalytic reaction. A number of techniques, including chemical reduction [3], thermal decomposition [12], physical vapor deposition [14], microemulsion method [15] and electrochemical deposition [16–19], have been developed to decrease the Pt loading in electrocatalyst while maintaining a high electrocatalytic activity. Of the various preparation methods, electrolytic deposition technique has unique advantages such as a high purity of deposit, easy-to-control procedure, and low cost of implementation [20,21]. It has been found [10,18,22–24] that there is a high electrocatalytic activity for the ammonia oxidation on the electrodeposited Pt electrode. For example, Yao and Cheng [18] fabricated Pt–Ni electrocatalysts with various Pt loadings by galvanostatic electrodeposition for electro-oxidation of ammonia. It was found that the electrocatalytic activity of the electrodeposited Pt–Ni electrode with only 1 mg cm^{-2} of Pt loading for the ammonia oxidation is comparable to that of pure Pt.

Furthermore, the Pt deposit is strongly dependent on the electrodepositing conditions, such as current density, depositing potential, solution concentration and additives [19,25]. It is thus expected [26–28] that there are essential effects of the electrodepositing parameters on the electrocatalytic activity of the prepared Pt catalyst for the ammonia oxidation.

In this work, the electrolytic deposition technique was used to prepare Pt electrocatalyst on a glass carbon substrate. The effects of the depositing current density and time on the surface morphology of the Pt electrocatalyst and its electrocatalytic activity for the ammonia oxidation were investigated by cyclic voltammetry and the scanning electron microscopy (SEM) characterization. The amount of Pt deposited was determined by an inductively coupled plasma method. For comparison, the electrocatalytic activity of a pure Pt electrode for the ammonia oxidation was measured.

* Corresponding author. Tel.: +86 21 34202981; fax: +86 21 34202981.
** Corresponding author. Tel.: +1 403 220 3693; fax: +1 403 282 8406.
E-mail addresses: wbhu@263.net (W.B. Hu), fcheng@ucalgary.ca (Y.F. Cheng).

0378-7753/$ – see front matter © 2011 Elsevier B.V. All rights reserved.
doi:10.1016/j.jpowsour.2011.05.058

2. Experimental

2.1. Preparation of Pt electrocatalysts

Pt electrocatalysts were electrodeposited galvanostatically on a glassy carbon (GC) substrate with 0.196 cm^2 in area as a function of various depositing current densities and times. The depositing electrolyte contained 0.5 M H_2SO_4, 5 mM H_2PtCl_6 and distilled water (ultra-high purity). All the chemicals were the analytic grade reagents. The electrolytic deposition of Pt was performed through a PARSTAT 2273 potentiostat/galvanostat system, where the GC was used as the working electrode, a platinum plate as the counter electrode, and a saturated calomel electrode (SCE) as the reference electrode.

2.2. Characterizations of the surface morphology and loading amount of Pt electrocatalysts

The surface morphology of the prepared Pt electrocatalyst was characterized using a SEM (JEOL, JSM-7600F). The amount of Pt depositing in the electrocatalyst was determined by an inductively coupled plasma (ICP) (Thermo Scientific, iCAP 6000) after dissolving Pt from the substrate.

2.3. Cyclic voltammogram measurements

The electrocatalytic activity of the prepared Pt electrocatalysts for the ammonia oxidation was investigated by cyclic voltammetry technique. The test solution contained 0.1 M ammonia and 1 M KOH. The cyclic voltammogram (CV) was measured at a potential sweep rate of 10 mV s^{-1}. The electroactive surface area of the Pt electrocatalyst was evaluated from the steady-state CV recorded at 50 mV s^{-1} in 0.5 M H_2SO_4 solution. Prior to and during the tests, the solution was deaerated with a high-purity Ar gas (99.999%). All tests were carried out at 25 ± 1 °C.

3. Results

3.1. Characterization of the surface morphology of the deposited Pt

Fig. 1 shows the SEM images of the surface morphologies of the prepared Pt electrocatalysts electrodepositing at 0.12 mA cm^{-2} for different depositing times, i.e., 3600s, 5400s and 7200s, respectively. The bright, spherical particles refer to the deposited Pt. It is seen that the amount and size of the deposited Pt increased remarkably with the depositing time. For example, the average size of Pt deposit was about 400 nm after depositing 3600s (Fig. 1a), while the average size increased to 780 nm after 7200s of deposition, as seen in Fig. 1c. Moreover, the deposited Pt tended to aggregate with the increasing time.

Fig. 2 shows the SEM images of the surface morphologies of the Pt electrocatalysts depositing at 0.3 mA cm^{-2} for 300 s, 600 s and 900 s, respectively. It is seen that, as the depositing time increases, the average size of the Pt particles increases from 60 nm to 200 nm. The particle aggregation becomes apparent as the time increases. Furthermore, it is seen that the deposited Pt particles were featured with somewhat 3-D cubic shape.

Fig. 3 shows the SEM images of the morphologies of the Pt electrocatalysts depositing at 0.6 mA cm^{-2} for 60 s, 120 s, 180 s and 240 s, respectively. Apparently, the morphology of the deposited Pt was quite different from those in Figs. 1 and 2. After 60 s of deposition (Fig. 3a), a large number of Pt particles with several tens of nm in size were dispersed on the GC substrate. When the depositing time increased to 120 s and 180 s, the Pt nanoparticles aggregated together to form a compact layer. This dendritic structure is more apparent when the depositing time increased to 240 s, as seen in Fig. 3d.

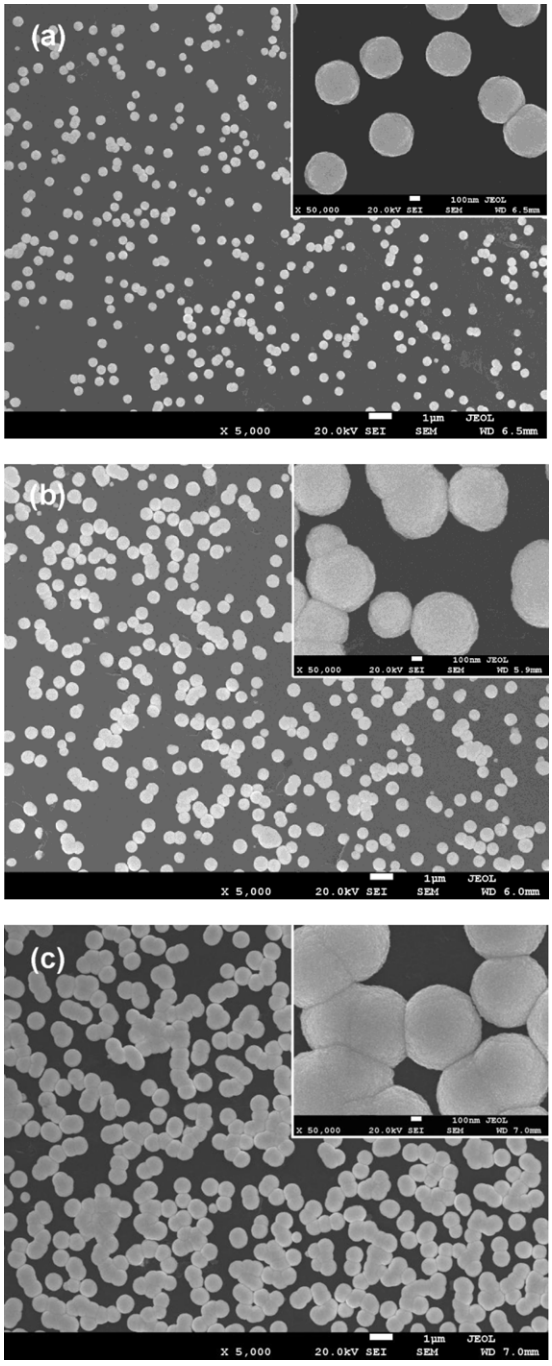

Fig. 1. SEM images of the surface morphologies of the Pt electrocatalysts electrodepositing at 0.12 mA cm^{-2} for (a) 3600, (b) 5400 and (c) 7200s, respectively.

Fig. 4 shows the SEM images of the morphologies of the Pt electrocatalysts depositing at a relatively high current density of 5 mA cm^{-2} for 5 s, 10 s, 30 s and 60 s, respectively. At such a high depositing current density, a layer of Pt particles could be formed on the GC surface over a quite short depositing time, such as 5 s (Fig. 4a), and the size of the particles was several nm to tens nm only. With the increase of the depositing time, the size of the Pt particles increased, and these particles became to agglomerate to form a film/layer. When the depositing time was up to 60 s, the formed Pt film exhibited a sheet-like dendritic morphology, as shown in

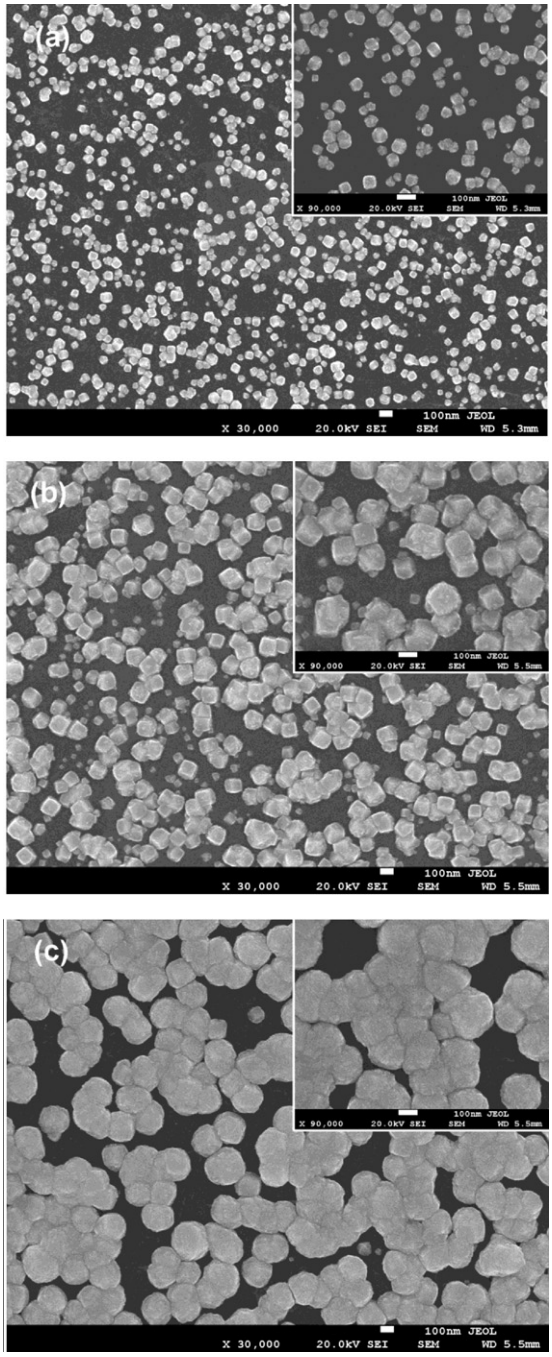

Fig. 2. SEM images of the surface morphologies of the Pt electrocatalysts electrodepositing at 0.3 mA cm^{-2} for (a) 300 s, (b) 600 s and (c) 900 s, respectively.

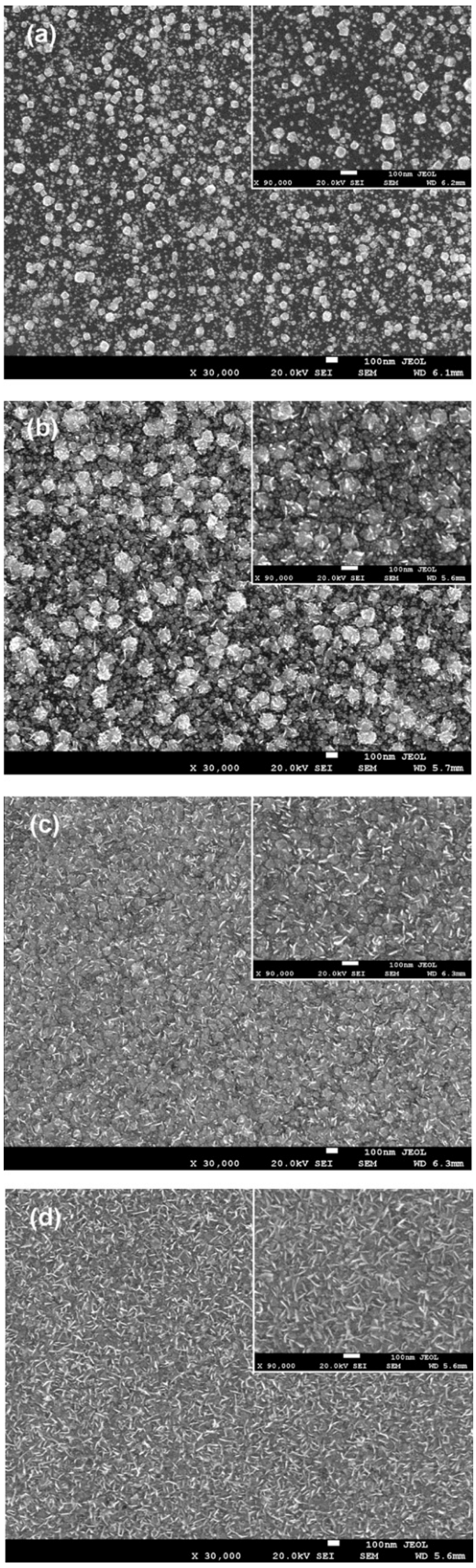

Fig. 3. SEM images of the surface morphologies of the Pt electrocatalysts electrodepositing at 0.6 mA cm^{-2} for (a) 60 s, (b) 120 s, (c) 180 s and (d) 240 s, respectively.

Fig. 4d, which was similar to that formed at 0.6 mA cm^{-2} after 240 s of deposition (Fig. 3d).

Table 1 shows the amount of Pt loadings determined by ICP under various depositing current densities and times, where the theoretical loading amount of Pt is calculated by Faraday's law assuming a 100% current efficiency. Apparently, the actual Pt loading increased with the depositing time at individual current density. Moreover, the actual Pt loading amount was obviously lower than the theoretical value, indicating a low depositing efficiency in reality. The depositing efficiency was up to about 70–75% when the deposition was carried out at a moderate current density of 0.6 mA cm^{-2}. However, when the depositing current density

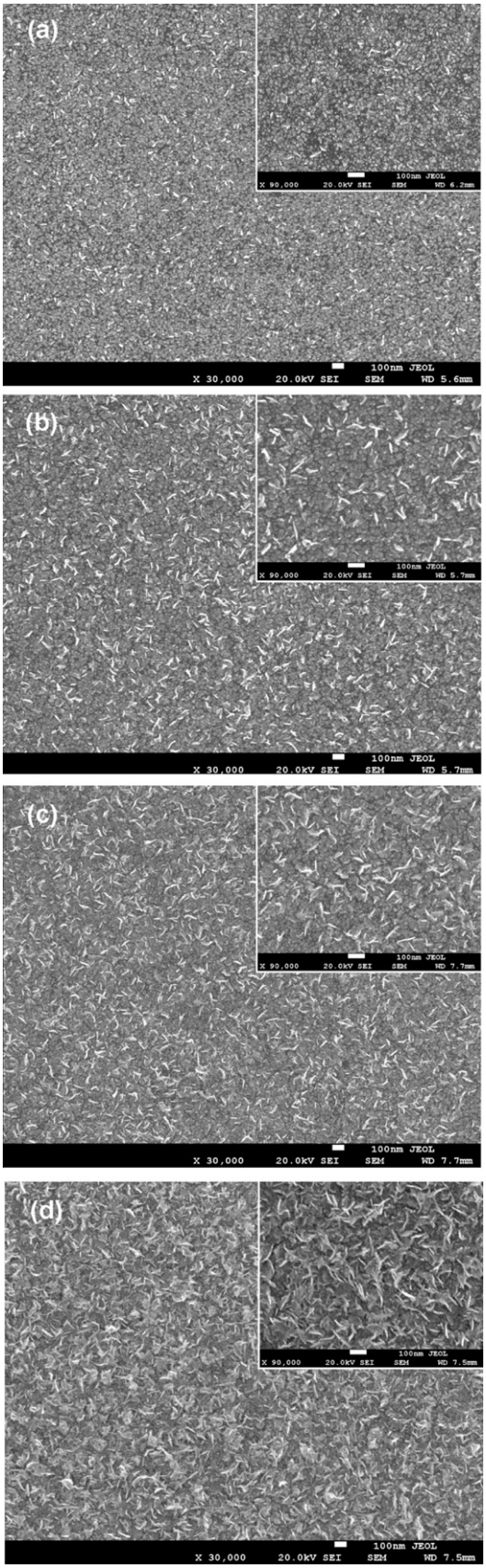

Fig. 4. SEM images of the surface morphologies of the Pt electrocatalysts electrodepositing at 5 mA cm^{-2} for (a) 5 s, (b) 10 s, (c) 30 s and (d) 60 s, respectively.

Table 1
Pt loadings determined by ICP analysis subject to various depositing current densities and times.

Depositing current density (mA cm^{-2})	Depositing time (s)	Theoretical Pt loading (μg cm^{-2})	Actual Pt loading (μg cm^{-2})	Deposition efficiency (%)
0.12	3600	229.3	42.2	18
0.12	5400	343.9	90.2	26
0.12	7200	458.6	181.3	40
0.3	300	47.8	19.6	41
0.3	600	95.5	53.9	56
0.3	900	143.3	99.0	69
0.6	60	19.1	13.4	70
0.6	120	38.2	27.2	71
0.6	180	57.3	43.1	75
0.6	240	76.4	54.2	71
0.6	300	95.5	66.8	70
5	5	12.7	7.0	55
5	10	25.5	10.5	41
5	30	76.4	19.1	25
5	60	152.9	39.3	26
5	90	229.3	55.5	24

increased to 5 mA cm^{-2}, the depositing efficiency reduced to about 20–50% only.

3.2. Measurements of cyclic voltammograms

Fig. 5 shows the CVs measured on pure Pt and the electrodeposited Pt at various depositing current densities and the Pt loading amount in 0.1 M ammonia + 1 M KOH solution. There was a similar feature for all CV plots, i.e., an anodic current peak observed at −0.38 V(SCE), which is attributed to the oxidation of ammonia to N_2 [12,13,17,18]. In the previous work [18], CV was measured in the absence of ammonia in the solution, and there was no characteristic current peak observed in the plot. Moreover, the CVs measured on the electrodeposited Pt electrodes showed a much higher peak current than that measured on the pure Pt electrode. At individual depositing current density, the anodic current density peak increased with the increasing Pt loading amount, while the characteristic peak potential was not shifted. Thus, the electrodeposited Pt contributes to the electrocatalytic oxidation of ammonia on the electrode. Furthermore, the peak current density also depended on the depositing current density. For example, the peak current density for the electrocatalyst depositing at 5 mA cm^{-2} with 7.0 μg cm^{-2} Pt loading was 0.81 mA cm^{-2} (Fig. 5e), which is comparable to the peak current density of 0.83 mA cm^{-2} measured on the Pt electrocatalyst depositing at a low current density of 0.12 mA cm^{-2} with a high Pt loading of 42.2 μg cm^{-2} (Fig. 5b).

4. Discussion

4.1. Effects of depositing current density on the morphology of Pt electrocatalysts

The mechanism of ammonia electro-oxidation on noble metals, such as platinum, proposed by Gerischer and Mauerer [29] involves the dehydrogenation step of $NH_{3,ads}$ to N_{ads} and the recombination of two $NH_{x,ads}$, where partially dehydrogenated species of $NH_{2,ads}$ and NH_{ads} are active intermediates to give the final product of N_2:

$$NH_3(aq) \rightarrow NH_{3,ads} \quad (1)$$

$$NH_{3,ads} + OH^- \rightarrow NH_{2,ads} + H_2O + e \quad (2)$$

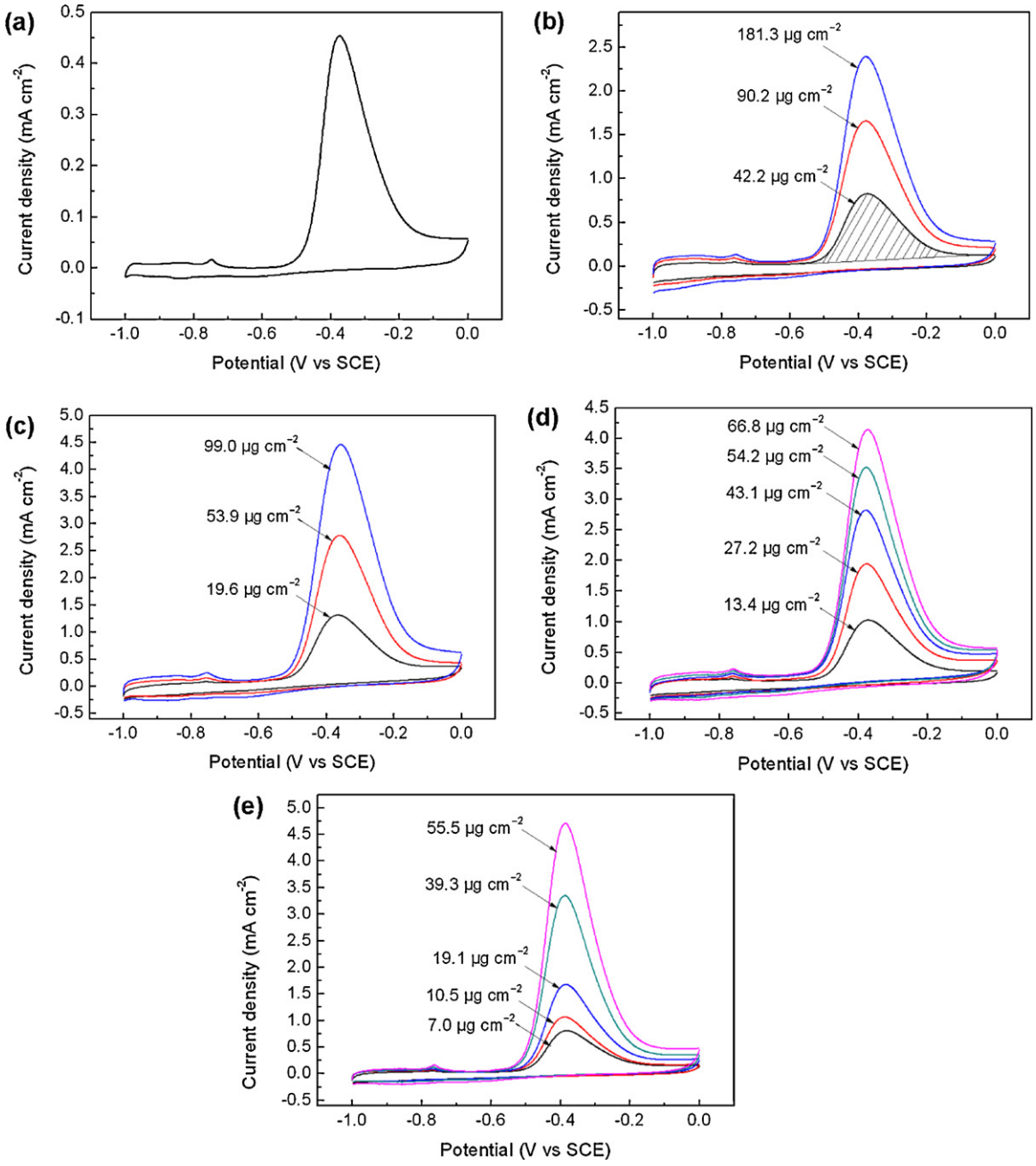

Fig. 5. Cyclic voltammograms measured on (a) pure Pt electrode, and the electrodeposited Pt depositing at (b) 0.12 mA cm^{-2}, (c) 0.3 mA cm^{-2}, (d) 0.6 mA cm^{-2} and (e) 5 mA cm^{-2} with different Pt loadings in 1 M KOH + 0.1 M ammonia solution.

$$NH_{2,ads} + OH^- \rightarrow NH_{ads} + H_2O + e \quad (3)$$

$$NH_{x,ads} + NH_{y,ads} \rightarrow N_2H_{x+y,ads} \quad (4)$$

$$N_2H_{x+y,ads} + (x+y)OH^- \rightarrow N_2 + (x+y)H_2O + (x+y)e \quad (5)$$

$$NH_{ads} + OH^- \rightarrow N_{ads} + H_2O + e \quad (6)$$

where $x = 1$ or 2, $y = 1$ or 2.

The anodic current peak in Fig. 5 may be the overlapped characteristic potential peaks of the three oxidation reactions as proposed.

The present work demonstrates that the surface morphology of the Pt electrocatalyst depends strongly on the electrodepositing conditions, i.e., the depositing current density and time. To understand the evolution of the surface morphology of Pt electrocatalyst during electrodeposition, chronopotentiometric responses during the galvanostatic electrodeposition of Pt at various depositing current densities are recorded and shown in Fig. 6. It is seen that the E–t curves show a strong dependence on the depositing current density. The initial drop of potential is possibly associated with the nucleation process [30]. After the initial induction period, the electrode potential becomes relatively stable with time. At a low deposition current density of 0.12 mA cm^{-2}, there is a quite long induction period of about 420 s (Fig. 6a). The induction time rapidly decreases to 100 s and 2 s at high current densities of 0.3 mA cm^{-2} (Fig. 6b) and 5 mA cm^{-2} (Fig. 6d), respectively. This indicates that the time for nucleation of Pt deposit decreases significantly with the increase of the depositing current density. Moreover, the steady-state potential shifts negatively.

Furthermore, there exists a correlation of the morphology of Pt deposit with the potential variation. At a low depositing current density of 0.12 mA cm^{-2}, the steady-state electrode poten-

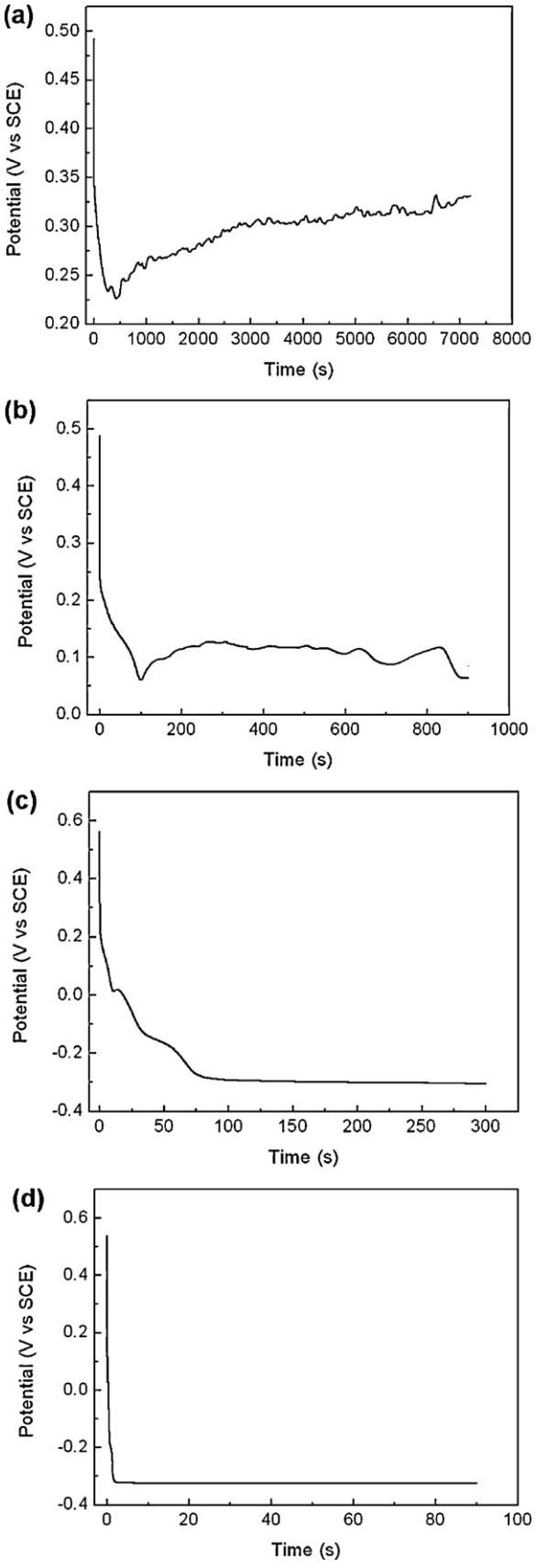

Fig. 6. Chronopotentiometric curves recorded during the galvanostatic electrodeposition of Pt at current densities of (a) 0.12 mA cm^{-2}, (b) 0.3 mA cm^{-2}, (c) 0.6 mA cm^{-2}, and (d) 5 mA cm^{-2}, respectively.

tial is maintained at a positive value between 0.23 V(SCE) and 0.32 V(SCE), and the Pt deposit is featured with a spherical morphology (Fig. 1). The increasing depositing time affects the size of the particle, but does not alter the morphological characteristics of Pt. When the depositing current density increases to 0.3 mA cm^{-2}, the steady-state potential decreases to 0.07 – 0.12 V(SCE), and some Pt particles exhibit cubic-like structure (Fig. 2a). As the applied current density further increases up to 0.6 mA cm^{-2}, the steady-state electrode potential decreases to −0.3 V(SCE), and small Pt nanosheets or tips are observed. When the depositing time extends to 240 s, the potential is stable at −0.3 V(SCE) and the Pt is characterized with a sheet-like dendritic structure (Fig. 3d). At a high current density of 5 mA cm^{-2}, the potential drops rapidly to a steady value of −0.32 V(SCE), and the nanosheets can be observed in the initial stage of the deposition process (Fig. 4a).

During electrodeposition, the mass transfer of Pt ions from the bulk solution through the diffusive layer towards the electrode surface (diffusion process) and the reduction reaction on the electrode (activation process) coexist. At the initial stage, Pt nuclei formed on the substrate surface undergo growth into small Pt particles (Figs. 1a, 2a, 3a and 4a). When the substrate electrode is at a positive potential, i.e., 0.23–0.32 V(SCE) in Fig. 6a, a limited current is provided for the Pt reduction, including its nucleation and growth. Thus, the depositing kinetics is activation-controlled, and the formed Pt particles exhibit a densely agglomerate structure, i.e., each spherical particle consists of a number of small Pt particles. When the electrode potential shifts negatively to −0.2 V(SCE) at high depositing current densities (Fig. 6b and c), the nucleation process is favored and the sites available for the Pt nucleation increase, resulting in an increasing density of Pt particles. The cubic-like structure of Pt is formed and is attributed to the hydrogen evolution occurring at relatively negative potentials [26,31]. As the electrode potential further decreases to −0.3 V(SCE), a large number of Pt ions are reduced in a short time period (Fig. 4a) under a large cathodic overpotential. The Pt deposition process switches to diffusion-controlled. As a consequence, the edge and corner of the Pt nuclei grow faster than other region, finally forming into Pt nanosheets. It was also reported [32] that the dendrite structure of the electrodeposited Pt is generally formed under mass transport controlling process. Moreover, the hydrogen evolution is significantly enhanced at the negative potential (−0.3 V(SCE)) and high current density (5 mA cm^{-2}). A low depositing efficiency is thus resulted in, as seen in Table 1.

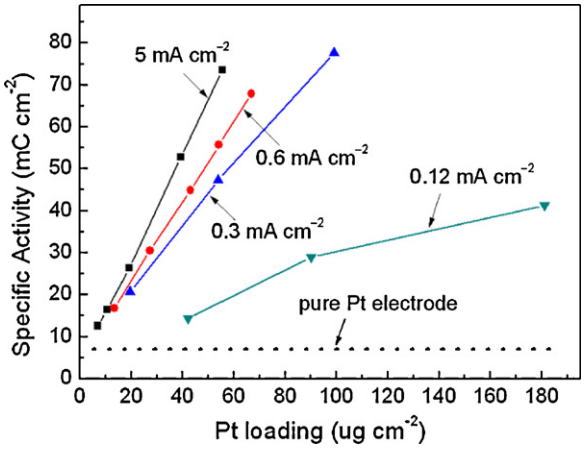

Fig. 7. Ammonia oxidation reaction activity under various Pt loadings. The four curves correspond to the different depositing current densities, and the dotted line is for the pure Pt electrode.

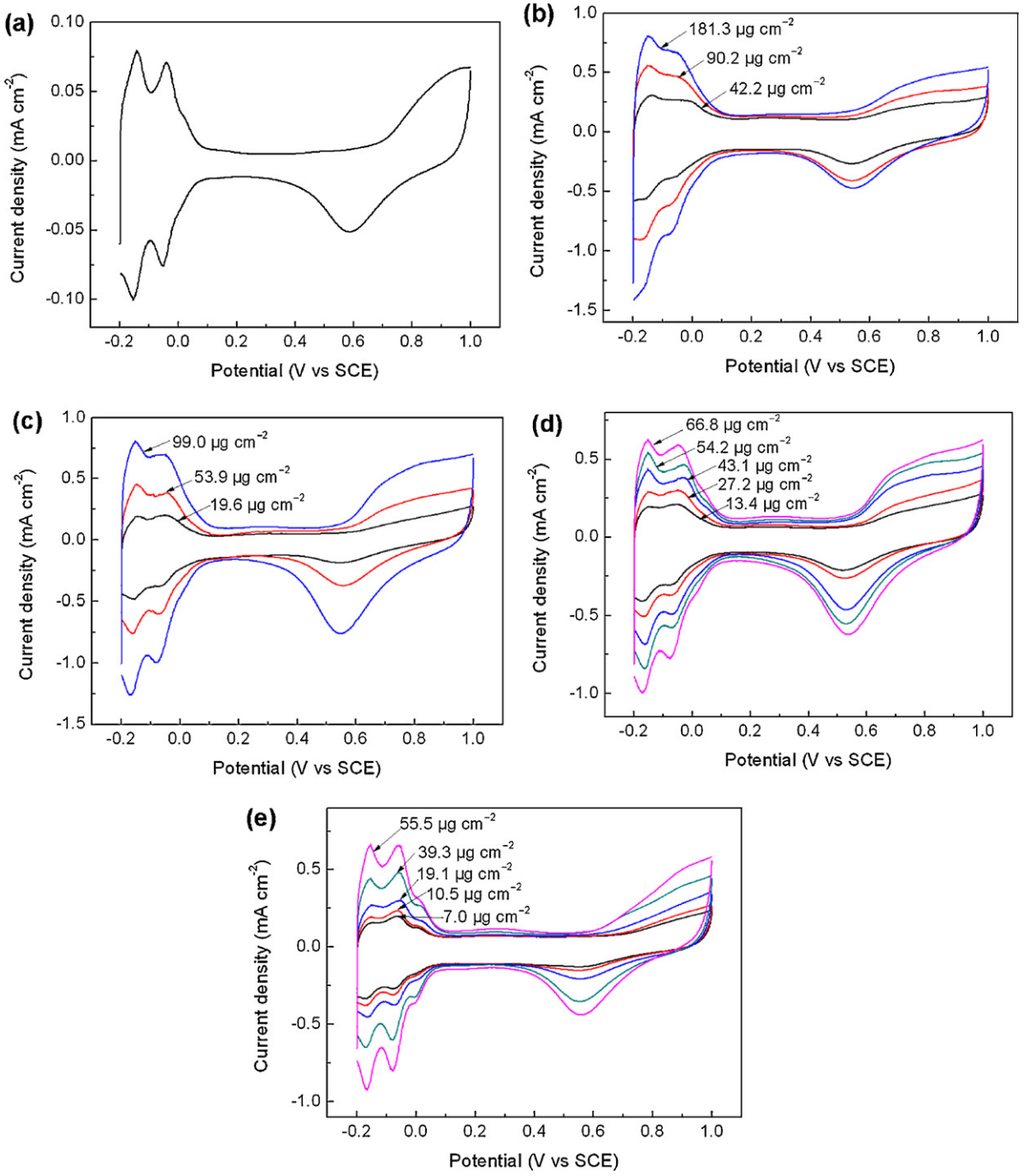

Fig. 8. Cyclic voltammograms measured on (a) pure Pt electrode and the prepared Pt electrocatalysts depositing at (b) 0.12, (c) 0.3, (d) 0.6 and (e) 5 mA cm^{-2} with different Pt loadings in 0.5 M H_2SO_4 solution.

4.2. Effect of depositing current density on the electrocatalytic activity of Pt electrocatalysts

The electrocatalytic activity of the prepared Pt electrocatalysts for oxidation of ammonia is determined by the charge required for the ammonia oxidation reaction (Q_{AOR}, mC cm^{-2}), which is determined as the area under the current peak in CV, such as the marked area in Fig. 5b.

Fig. 7 shows the electrocatalytic activity expressed as Q_{AOR} of the Pt electrocatalysts with various Pt loadings for the ammonia oxidation, where the four curves correspond to the different depositing current densities, and the dotted line is for the pure Pt electrode. It is seen that the electrodeposited Pt catalysts have much higher electrocatalytic activity than pure Pt. The prepared Pt electrocatalysts with very low loading (7.0–181.3 μg cm^{-2} depending on the depositing current density) could achieve the electrocatalytic activity comparable to the pure Pt electrode. Moreover, the electrocatalytic activity of the prepared Pt catalyst increases continuously with the Pt loading, which depends strongly on the depositing current density. For example, the electrocatalytic activity of Pt catalyst with 39.3 μg cm^{-2} loading electrodepositing at 5 mA cm^{-2} is 52.8 mC cm^{-2}, which is about 3.7 times of that with 42.2 μg cm^{-2} Pt loading depositing at 0.12 mA cm^{-2}.

According to the morphological analysis previously, the influence of the depositing current density on the electrocatalytic activity of Pt is associated with the morphological change. High

depositing current densities result in Pt particles with a small size after a short time period of deposition or a sheet-like dendritic structure with a long depositing time. This typical morphological feature contributes to high specific electrocatalytic activities. At low depositing current densities, the spherical Pt particles with a large size from 400 nm to 780 nm have the low electrocatalytic activity. To understand mechanistically the effect of the morphological feature on the electrocatalytic activity of Pt, the electroactive surface area as a function of morphology of the deposited Pt electrocatalysts is discussed as follows.

4.3. Electroactive surface area of Pt electrocatalysts

The electroactive surface area (ESA) of the prepared Pt electrocatalysts is determined by measurement of CVs in 0.5 M H_2SO_4 solution at a scan rate of 50 mV s^{-1}. Fig. 8 shows the CVs measured on pure Pt and the Pt electrocatalysts with various Pt loadings at various current densities. All CVs show typical potential regions for the hydrogen adsorption/desorption (−0.2 V(SCE) to 0.1 V(SCE)), the double layer potential region (0.1–0.5 V(SCE)), and the formation/reduction of the surface Pt oxide, Pt–OH_{ad} (0.5–1.0 V(SCE)). The hydrogen desorption peaks at −0.15 V(SCE) and −0.05 V(SCE) in the anodic branch are typically attributed to the desorption of the weakly and strongly bonded hydrogen species, respectively [33]. The current density for the hydrogen desorption increases with the Pt loading, indicating the increasing ESA. It is found that the electrodeposited Pt shows a much higher hydrogen desorption current density than that of pure Pt, indicating that the former has a much larger electroactive surface area.

The ESA of Pt electrocatalyst is calculated from the CVs according to the following equation [20]:

$$\mathrm{ESA} = \frac{Q_H}{Q_H^0 S_g} \tag{7}$$

where Q_H is the charge for the hydrogen desorption (mC), Q_H^0 is the specific charge for a hydrogen monolayer on Pt (0.21 mC cm^{-2}) [34], and S_g is the apparent geometric area (cm^2). The Q_H value for the individual electrocatalyst can be calculated by integrating the area corresponding to the hydrogen desorption by subtracting the double layer contribution.

Fig. 9 shows the ESA of Pt electrocatalysts with various Pt loadings at different depositing current densities. For comparison, the ESA of a pure Pt electrode is also given. It is seen that the ESA of the electrodeposited Pt catalysts, ranging from 2.0 to 12.5 cm^2 cm^{-2}, increases continuously with the Pt loading. Apparently, the true electroactive surface area is much higher than the apparent geometric area of the electrode. Moreover, the ESA of the pure Pt electrode is 1.1 cm^2 cm^{-2}, which is only 10% higher than its geometric area. The determined ESA demonstrates that the electrodeposited Pt has a higher ESA per geometric area than the pure Pt electrode, and thus contributes to a higher electrocatalytic activity for the ammonia oxidation. Moreover, the ESA is dependent on the depositing current density. For instance, for ESA between 6.6 and 7.4 cm^2 cm^{-2}, a 90.2 μg cm^{-2} Pt is required for the electrocatalyst depositing at 0.12 mA cm^{-2}, while only 39.3 μg cm^{-2} Pt is required for that depositing at 5 mA cm^{-2}. Therefore, at individual Pt loading amount, there is a lower electroactive area for electrocatalyst fabricated at a lower current density than that deposited at a higher current density.

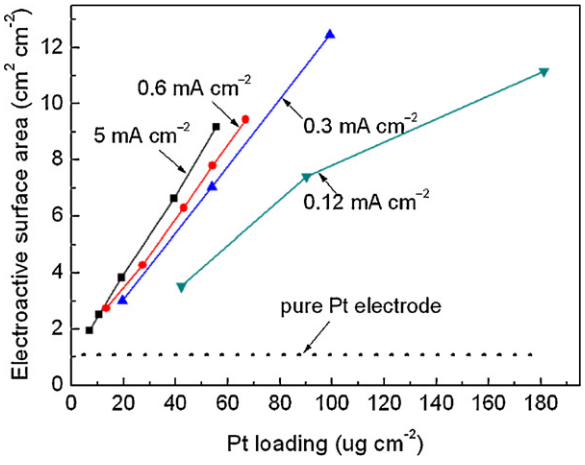

Fig. 9. Electroactive surface areas under various Pt loadings depositing at different current densities, and the dotted line corresponds to the electroactive surface area of the pure Pt electrode.

5. Conclusions

The electrocatalytic activity of the electrodeposited Pt for the ammonia oxidation is dependent on the depositing current density and time. Under the investigated conditions, the electrodeposited Pt has much higher electrocatalytic activity than the pure Pt electrode due to a high electroactive surface area of the Pt deposit.

The electrocatalytic activity of the Pt catalyst is improved with the increase of the Pt loading. Moreover, the electrocatalytic activity of Pt increases with the depositing current density which results in an increasing Pt loading amount.

Furthermore, the effect of the depositing current density on the electrocatalytic activity of Pt also depends on its surface morphology which is affected by the deposition current density. The high depositing current density generates small Pt particles at nanometer scale within a short depositing time period, or sheet-like dendritic structure over a long period of deposition. However, the low depositing current density leads to large Pt particles at several hundreds of nanometer with a relatively smooth morphology. The Pt electrocatalyst with the former morphological feature exhibits a higher electrocatalytic activity than the later due to the higher electroactive surface area.

Acknowledgements

The authors thank Drs. S. Xu and Y.J. Zhou in the Instrumental Analysis Center of Shanghai Jiao Tong University for the ICP analysis. This work was supported by the National Natural Science Foundation of China (50474004 and 51004070), Shanghai Jiao Tong University (S050IPP001003 and T050PRP18010), and Canada Research Chairs Program.

References

[1] F. Vitse, M. Cooper, G.G. Botte, J. Power Sources 142 (2005) 18.
[2] B.K. Boggs, G.G. Botte, J. Power Sources 192 (2009) 573.
[3] F.J. Vidal-Iglesias, J. Solla-Gullón, V. Montiel, J.M. Feliu, A. Aldaz, J. Power Sources 171 (2007) 448.
[4] F.J. Vidal-Iglesias, J. Solla-Gullón, V. Montiel, J.M. Feliu, A. Aldaz, J. Phys. Chem. B 109 (2005) 12914.
[5] A. Kapałka, A. Cally, S. Neodo, C. Comninellis, M. Wächter, K.M. Udert, Electrochem. Commun. 12 (2010) 18.
[6] R. Metkemeijer, P. Achard, J. Power Sources 49 (1994) 271.
[7] K. Kordesch, J. Gsellmann, M. Cifrain, S. Voss, V. Hacker, R.R. Aronson, C. Fabjan, T. Hejze, J. Daniel-Ivad, J. Power Sources 80 (1999) 190.
[8] G. Strickland, Int. J. Hydrogen Energy 9 (1984) 759.
[9] E.P. Bonnin, E.J. Biddinger, G.G. Botte, J. Power Sources 182 (2008) 284.
[10] M. Cooper, G.G. Botte, J. Electrochem. Soc. 153 (2006) A1894.
[11] A.C.A. de Vooys, M.T.M. Koper, R.A. van Santen, J.A.R. van Veen, J. Electroanal. Chem. 506 (2001) 127.
[12] K. Endo, K. Nakamura, Y. Katayama, T. Miura, Electrochim. Acta 49 (2004) 2503.
[13] K. Endo, Y. Katayama, T. Miura, Electrochim. Acta 49 (2004) 1635.
[14] K. Yamada, K. Miyazaki, S. Koji, Y. Okumura, M. Shibata, J. Power Sources 180 (2008) 181.

[15] J. Solla-Gullón, V. Montiel, A. Aldaz, J. Clavilier, J. Electroanal. Chem. 491 (2000) 69.
[16] C. Paoletti, A. Cemmi, L. Giorgi, R. Giorgi, L. Pilloni, E. Serra, M. Pasquali, J. Power Sources 183 (2008) 84.
[17] T. Katan, R.J. Galiotto, J. Electrochem. Soc. 110 (1963) 1022.
[18] K. Yao, Y.F. Cheng, J. Power Sources 173 (2007) 96.
[19] H. Jeon, J. Joo, Y. Kwon, S. Uhm, J. Lee, J. Power Sources 195 (2010) 5929.
[20] F. Gloaguen, J.M. Leger, C. Lamy, A. Marmann, U. Stimming, R. Vogel, Electrochim. Acta 44 (1999) 1805.
[21] H. Kim, N.P. Subramanian, B.N. Popov, J. Power Sources 138 (2004) 14.
[22] K. Yao, Y.F. Cheng, Int. J. Hydrogen Energy 33 (2008) 6681.
[23] L. Zhou, Y.F. Cheng, M. Amrein, J. Power Sources 177 (2008) 50.
[24] B.K. Boggs, G.G. Botte, Electrochim. Acta 55 (2010) 5287.
[25] F.J. Rodriguez Nieto, M.A. Pasquale, C.R. Cabrera, A.J. Arvia, Langmuir 22 (2006) 10472.
[26] J.L. Zubimendi, G. Andreasen, W.E. Triaca, Electrochim. Acta 40 (1995) 1305.
[27] F.J. Vidal-Iglesias, J. Solla-Gullón, P. Rodrıĭguez, E. Herrero, V. Montiel, J.M. Feliu, A. Aldaz, Electrochem. Commun. 6 (2004) 1080.
[28] M. Subhramannia, V.K. Pillai, J. Mater. Chem. 18 (2008) 5858.
[29] H. Gerischer, A. Mauerer, J. Electroanal. Chem. 25 (1970) 421.
[30] Y. Li, G.Q. Shi, J. Phys. Chem. B 109 (2005) 23787.
[31] S. Garbarino, A. Ponrouch, S. Pronovost, J. Gaudet, D. Guay, Electrochem. Commun. 11 (2009) 1924.
[32] W.C. Ye, J.F. Yan, Q.A. Ye, F. Zhou, J. Phys. Chem. C 114 (2010) 15617.
[33] N.M. Markovic, P.N. Ross, Surf. Sci. Rep. 45 (2002) 117.
[34] E. Antolini, L. Giorgi, A. Pozio, E. Passalacqua, J. Power Sources 77 (1999) 136.